Modeling the Thermal Conductivity of Hydrofluorocarbons, Hydrofluoroolefins and their Binary Mixtures using Residual Entropy Scaling and Cubic-plus Association Equation of State

Hangtao Liu, Fufang Yang, Xiaoxian Yang, Zhen Yang, Yuanyuan Duan

Modeling the thermal conductivity of hydrofluorocarbons, hydrofluoroolefins and their binary mixtures using residual entropy scaling and cubic-plus-association equation of state

Hangtao Liu [a], Fufang Yang [a,b,d], Xiaoxian Yang [c], Zhen Yang [a], Yuanyuan Duan [a,*]

[a] Key Laboratory for Thermal Science and Power Engineering of Ministry of Education, Beijing Key Laboratory for CO_2 Utilization and Reduction Technology, Tsinghua University, Beijing 100084, China
[b] Center for Energy Resources Engineering (CERE), Department of Chemical and Biochemical Engineering, Technical University of Denmark, 2800 Kgs. Lyngby, Denmark
[c] Fluid Science & Resources Division, Department of Chemical Engineering, University of Western Australia, Crawley, WA 6009, Australia
[d] IFP Energy Nouvelles, 1 et 4 Avenue de Bois-Préau, 92852 Rueil-Malmaison Cedex, France

Thermal conductivity strongly impacts heat transfer, and thus is an important thermophysical property for refrig-eration and medium-low-temperature heat utilization systems. In this work, the residual entropy scaling incorpo-rating cubic-plus-association equation of state, as a convenient and robust modeling approach for the transport properties of pure and mixture fluids of which the experimental data are scarce or unavailable, is extended to the thermal conductivity of hydrofluorocarbons, hydrofluoroolefins, and their binary mixtures. For all the investi-gated pure and mixture fluids, the dependence of the thermal conductivity on the thermodynamic state is reduced to a 'universal' univariate function of the rescaled residual entropy with one adjustable parameter for each pure fluid and no further adjustable parameter for mixtures. A new formulation of the reference thermal conductivity is proposed to improve the accuracy for the binary mixtures. The model reproduces the thermal conductivity of the investigated pure and mixture fluids with the root mean squared deviation of 2.9% in gas, liquid, and super-critical regions. The lack or uneven distribution of the data is overcome based on the residual entropy scaling with the extensive data of R134a as a reference.

Nomenclature

f^{int}
A dimensionless correction factor in Eq. (4)
k_B
Boltzmann constant, 1.380649×10^{-23} J·K^{-1}
m
Molecular mass
N
Number of data points
p
Pressure
R
Universal gas constant, 8.314462618 J·mol^{-1}·K^{-1}
s
Entropy
T
Temperature
v
Molar volume
x
Molar fraction

Greek Symbols

δ
Percentage deviation of the model from the experimental data
ε
A Lennard-Jones parameter for dilute-gas viscosity calculation
ζ
Rescaling parameter for residual entropy in the thermal conductivity model

η
Viscosity
λ
Thermal conductivity
λ^{ref}
Reference thermal conductivity for scaling
ξ
Rescaling parameter for residual entropy in the viscosity model
ρ
Density
ρ_N
Number density
σ
A Lennard-Jones parameter for dilute-gas viscosity calculation

Subscript

cal
Calculated data
cr
Critical property
exp
Experimental data
max
Maximum
mix
Mixture property
nb
Normal boiling point property

Superscript

CE
Translation term calculated by the Chapman-Enskog solution
ig
Ideal-gas property
int
Internal term
o
Dilute-gas property
res
Residual property
*
Reduced value

1. Introduction

As the cornerstones for economic and conceptual optimization, the thermophysical properties of hydrofluorocarbons (HFCs) and hydrofluoroolefins (HFOs) have developed with their wide use as working fluids in refrigeration [1] and medium-low-temperature heat utilization including heat pump and organic Rankine cycle [2–5]. Current research interests are increasingly focusing on replacing pure HFCs and HFOs with their mixtures for better performance [6]. However, both experimental and modeling studies on the mixtures are challenging tasks and rare for the HFC/HFO mixtures. In this context, a semi-theoretical model, which only requires a small quantity of experimental data and can be easily extended to mixtures, could be one of the most feasible approaches to evaluate the thermophysical properties. In our recent-developed models, the cubic-plus-association (CPA) equation of state was applied to HFCs, HFOs, and their binary mixtures [7] with the association term accounting for the weak hydrogen bond of the CH···F interaction, and then extended to the viscosity calculation using the residual entropy scaling (RES) approach [8,9]. With simple mathematical formulations and only 5 parameters for the thermodynamic properties and 1 parameter for the viscosity, the models reproduce the thermodynamic and viscosity experimental data of the investigated fluids accurately in both gas and liquid phases. Thermal conductivity is an important thermophysical property that strongly impacts the heat transfer of working fluids in the components and pipelines. Therefore, it is necessary to further extend the models to thermal conductivity.

Thermal conductivity has been modeled by various semi-theoretical approaches as well as empirical correlations using data from measurements [10] or simulations [11]. The extended corresponding state (ECS) model [12–14] is the current state-of-the-art semi-theoretical model to estimate the thermal conductivity of HFCs and HFOs. The estimations are made through the conformal transformation of the fluid of interest onto a reference fluid, for which accurate thermodynamic and thermal conductivity models are available. There are also semi-theoretical models based on physical assumptions on the mechanism of thermal conduction, e.g., the hard-sphere model [15,16] and the vibrational theory [17], which estimate the thermal conductivity from the perspective of molecular collisions and vibrations, respectively. All these models are isolated theoretical frameworks that link the thermal conductivity and thermodynamic states, while the RES approach, proposed by Rosenfeld [18,19], reveals the link between the transport properties and thermodynamic states by a univariate function of residual entropy. The residual entropy can be calculated with an equation of state, which usually has solid theoretical and experimental foundations due to the existence of the thermodynamic property relations. Therefore, with the aid of a well-developed equation of state, the RES approaches have the potential to provide more accurate and more robust predictions of transport properties than the isolated-theory-based models. Having been successfully applied to the viscosity of HFCs, HFOs, and their binary mixtures [8,9], our RES model incorporating CPA equation of state will be extended to the thermal conductivity in this work.

In the viscosity model [8,9], the reduced viscosity, i.e., viscosity divided by a reference value, shows a good univariate dependence on residual entropy in the wide fluid region with the dilute gas viscosity adopted as the reference value. However, the thermal conductivity divided by the dilute gas thermal conductivity does not show as good a scaling performance in the dense region for HFCs/HFOs. Various formulations of reduced thermal conductivity were applied to the RES models of Lennard-Jones [20,21] and molecular fluids [22–26]. For the mixtures of HFCs/HFOs, the approaches applicable for pure fluids may deviate from experimental results. Therefore, it is essential to reconsider the reference thermal conductivity for the pure and mixture fluids. Besides, the experimental data of thermal conductivity usually have larger relative uncertainty than those of viscosity [27]. Therefore, a more detailed evaluation is needed.

In this work, a RES model is applied to 15 HFCs/HFOs and their binary mixtures. The thermodynamic properties are determined using our recently-tailored CPA equation of state [7]. First, the CPA equation of state and RES model are briefly introduced. To obtain a better scaling performance, the formulation of reference thermal conductivity for the pure fluids is dis-

cussed. Then, a 'universal' correlation of the reduced thermal conductivity as a function of residual entropy is fitted with R134a, which has the most extensive experimental data among the investigated fluids, and then applied to other pure fluids by introducing only one adjustable parameter. Finally, the model is extended to the binary mixtures based on the mixing/combining rules of the CPA equation of state and the newly-proposed reference thermal conductivity. The experimental data of the binary mixtures are taken as the reference only for model validation because no additional mixture-specific parameter is introduced in the mixture model. In our previous study on the viscosity RES model [8,9], the model range was conservatively restricted to the subcritical region. In contrast, the thermal conductivity RES model in the present work is applied to both the sub- and supercritical region.

2. Methods

This section introduces the CPA equation of state, RES model, and fitting procedure of the RES correlation and its extending to the mixtures. The method is applied to 12 HFCs, 3 HFOs, and their binary mixtures as listed in Fig. 1 with the number of selected data for each fluid. Similar to viscosity and thermodynamic properties, extensive thermal conductivity data covering the whole range of thermodynamic state of interest are not available for most of the fluids. Moreover, the experimental data for most of the binary mixtures remains unreported. This is also what motivates us to develop a semi-theoretical model.

2.1. Cubic-plus-association equation of state

In the RES model, the dependence of the thermal conductivity on the thermodynamic state is represented by the residual entropy. The accuracy of the residual entropy calculation has a significant impact on the scaling performance. Therefore, it is necessary for the equation of state to yield a faithful representation of the residual entropy as well as the volumetric and vapor-liquid-equilibria properties. In this work, we adopt the CPA equation of state, which was developed by Kontogeorgis et al. [28,29] and recently-tailored for the investigated fluids [7], to calculate the residual entropy. The model uses a revised alpha function that satisfies the thermodynamic consistency criterions [30].

The effect of the weak hydrogen bond is represented by the association term of the CPA equation of state. The accuracy in both gas and liquid phases was taken into account in the fitting procedure. Thus, the CPA equation of state can reproduce the volumetric and the vapor-liquid-equilibria properties in both gas and liquid phases. Its successful application with the RES model on the viscosity prediction demonstrates its reliability for the residual entropy calculation. Readers can refer to our previous work [7] for the details of the CPA equation of state.

2.2. Residual entropy scaling

Rosenfeld [18,19] proposed the quasi-universal corresponding-state relationship for the dimensionless transport properties as a function of the 'excess entropy'. The relationship was verified by the simulation results of the dense model fluids, e.g., hard-sphere, soft-sphere, Lennard-Jones, and then applied to the real fluids.

The independent variable 'excess entropy' used by Rosenfeld [18,19] is equivalent to the residual entropy in the present work according to the tradition of equilibrium thermodynamics. It is defined as the difference between the entropy and its ideal gas contribution at the same temperature and density,

$$s^{\mathrm{res}}(T,\rho) = s^{\mathrm{ig}}(T,\rho) - s(T,\rho) \tag{1}$$

where T is temperature, ρ is density, s^{res} is residual entropy, s^{ig} is ideal gas entropy, and s is entropy. Readers can refer to our previous work [7] for the derivations of the residual entropy from the CPA equation of state. For convenience, the formulations are also provided in the supplementary materials.

The reduced thermal conductivity, λ^*, was originally defined by [19].

$$\lambda^* = \frac{\lambda}{\lambda^{\mathrm{ref}}} = \frac{\lambda}{\rho_{\mathrm{N}}^{2/3}\sqrt{k_{\mathrm{B}}^3 T/m}} \tag{2}$$

where λ is thermal conductivity, ρ_{N} is number density in unit of m^{-3}, k_{B} is the Boltzmann constant, and m is the mass of the fluid molecule. It was proposed to make the thermal conduc-

Number of data	R1243zf	R1234ze(E)	R1234yf	R245fa	R245ca	R236fa	R236ea	R227ea	R161	R152a	R143a	R134a	R125	R32	R23
R23	0	0	0	0	0	0	0	0	0	0	0	0	0	0	320
R32	37	0	36	0	0	0	0	0	0	0	0	1425	453	999	
R125	0	12	12	0	0	0	0	0	0	11	162	1160	1673		
R134a	0	12	12	0	0	0	0	0	0	0	0	6271			
R143a	0	12	12	0	0	0	0	0	0	0	539				
R152a	0	0	0	0	0	0	0	0	0	1734					
R161	0	0	0	0	0	0	0	0	361						
R227ea	0	0	0	0	0	0	0	291							
R236ea	0	0	0	0	0	0	202								
R236fa	0	0	0	0	0	256									
R245ca	0	0	0	0	131										
R245fa	0	0	0	555											
R1234yf	0	12	744												
R1234ze(E)	0	1102													
R1243zf	35														

Fig. 1. Investigated fluids and the numbers of selected experimental data (blue: pure fluids; orange: binary mixtures).

tivity dimensionless and proved useful for the scaling of dense fluids. Thus, we can model the thermal conductivity by correlating the univariate function $\lambda^* = \lambda / \lambda^{\mathrm{ref}} = f(s^{\mathrm{res}})$.

To avoid the divergence of the reduced thermal conductivity at the ideal gas limit ($s^{\mathrm{res}} = 0$, $\rho_{\mathrm{N}} \to 0$), the dilute gas thermal conductivity is one of the candidates to replace λ^{ref} in Eq. (2). The Chapman-Enskog solution yields the thermal conductivity of the monatomic dilute gas according to the kinetic theory as

$$\lambda^{\mathrm{o,CE}} = \eta^{\mathrm{o}} \cdot \frac{15R}{4M} \tag{3}$$

where η^{o} is viscosity of dilute gas, R is universal gas constant, and M is molar mass. The Chapman-Enskog solution and the collision integral correlations proposed by Neufeld et al. [31] yield the equations of dilute gas viscosity, as included in our previous work [8] and the supplementary materials. For polyatomic gas, the internal (i.e., rotational or vibrational) degrees of freedom also contribute to the thermal conductivity, which is different from the case of viscosity. The internal contribution can be obtained following the modified Eucken correlation,

$$\lambda^{\mathrm{o,int}} = f^{\mathrm{int}} \eta^{\mathrm{o}} \cdot \frac{c_p^{\mathrm{o}} - 2.5R}{M} \tag{4}$$

where f^{int} is a dimensionless factor with a value of about 1.32 in theory for the Lennard-Jones fluid, c_p^{o} is the ideal gas specific heat. Thus, the dilute gas thermal conductivity is represented by the sum of the translational and internal terms,

$$\lambda^{\mathrm{o}} = \lambda^{\mathrm{o,CE}} + \lambda^{\mathrm{o,int}} \tag{5}$$

For more accurate estimation, the factor f^{int} in Eq. (4), or more directly, the dilute gas thermal conductivity λ^{o} as a whole, can be correlated as a function of temperature using the dilute gas thermal conductivity data (if available).

Both $\lambda^{\mathrm{o,CE}}$ and λ^{o} can be adopted as the reference thermal conductivity for real fluids. Fig. 2 compares the performance: the approach using $\lambda^* = \lambda / \lambda^{\mathrm{o,CE}}$ shows overall good scaling performance but fails in the ideal gas limit, while the approach using $\lambda^* = \lambda / \lambda^{\mathrm{o}}$ collapses in the ideal gas limit but scatters at large residual entropy. Therefore, in the reference term, the

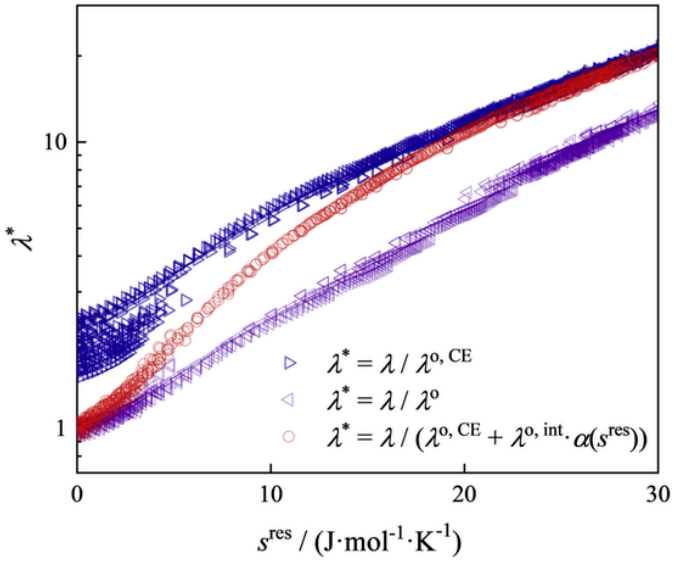

Fig. 2. The comparison of the reduced thermal conductivity for R32 as a function of residual entropy.

contribution of internal degrees of freedom of dilute gas is supposed to be completely included in the ideal gas limit and decrease in the dense region. Hopp et al. [22] introduced an empirical transition function $\alpha(s^{\mathrm{res}})$ into the formulation of the reference thermal conductivity,

$$\lambda^{\mathrm{ref}}\left(T, s^{\mathrm{res}}\right) = \lambda^{\mathrm{o,CE}}(T) + \lambda^{\mathrm{o,int}}(T) \cdot \alpha\left(s^{\mathrm{res}}\right) \tag{6}$$

In this work, the transition function is defined as

$$\alpha\left(s^{\mathrm{res}}\right) = \exp\left(-s^{\mathrm{res}}/R\right) \tag{7}$$

to make the internal term completely included in the ideal gas limit and vanish gradually with the increasing s^{res}. Substituting Eq. (6) to Eq. (2), the reduced thermal conductivity shows a univariate function dependence on the residual entropy in both the ideal gas limit and the dense region, as shown in Fig. 2 with the red circle dots.

To account for the real temperature dependence of the dilute gas thermal conductivity of the investigated pure fluids, we correlate the factor f^{int} in Eq. (4) as a polynomial in temperature for each fluid

$$f^{\mathrm{int}} = c_0 + c_1 T + c_2 T^2 \tag{8}$$

where the coefficients are listed in Table 1. The normal boiling points and critical parameters for the 15 HFCs and HFOs are also provided in Table 1. Readers can refer to the supplementary materials for the parameters of the CPA equation of state and dilute gas thermal conductivity model. The ideal gas specific heat c_p^0, with the data generated by NIST REFPROP 10.0 [32], is also correlated as a polynomial in temperature, of which the coefficients are listed in the supplementary materials for readers' convenience.

2.3. Correlation

To obtain an accurate semi-theoretical model, one needs to select the datasets before moving on to correlation. Since the dependence of thermal conductivity on thermodynamic state can be reduced to a univariate function of residual entropy, the outliers or the conflicting data can be instantly identified in the λ^*-s^{res} plot of experimental data. For the conflicting data, the sources, experimental techniques, and reported uncertainties are considered for determining which set to use. The datasets or data points may also be excluded because they are not suitable for the present purpose or that they overlap with other datasets. The present work has no intention to critically evaluate experimental literature. Exclusion of experimental datasets does not indicate the authors' recommendation against them in other occasions. Table 2 shows an overview of the experimental data of each fluid in the correlation. For detailed information on the experimental data, please refer to Table S6 in the supplementary materials.

Fig. 3 (a) shows the reduced thermal conductivity data against the residual entropy. For each of the investigated fluids, the reduced thermal conductivity shows good scaling performance (following a perfect univariate function of residual entropy). The curves of the 15 pure fluids are close but not exactly the same. The similarity results from the common features of molecular structure and intermolecular interaction of these compounds. The slight differences result from their 'personalities' in the extent of these features. Considering these differences, a straightforward idea is to fit the model parameters separately for each fluid. However, the experimental data

Table 1
Parameters of pure fluids.

Fluid	Full name	T_{nb} / K	T_{cr} / K	p_{cr} / MPa	ζ	Coefficients of Eq. (8) for f^{int}		
						c_0	c_1 / (10^{-3} K)	c_2 / (10^{-5} K)
R23	Trifluoromethane	191.132	299.293	4.832	0.9668	0.9185	0.5428	0
R32	Difluoromethane	221.499	351.255	5.782	0.9338	1.8677	−6.8437	1.2489
R125	Pentafluoroethane	225.06	339.173	3.6177	0.9729	1.2068	0.4480	0
R134a	1,1,1,2-Tetrafluoroethane	247.076	374.21	4.05928	1.0000	−0.0335	6.8865	−0.8000
R143a	1,1,1-Trifluoroethane	225.91	345.857	3.761	0.9554	1.0737	0.8267	0
R152a	1,1-Difluoroethane	249.127	386.411	4.51675	0.9933	0.2737	5.2905	−0.6282
R161	Fluoroethane	235.614	375.25	5.046	0.9767	−3.5570	27.1202	−3.7842
R227ea	1,1,1,2,3,3,3-Heptafluoropropane	256.81	374.9	2.925	0.9975	0.9504	1.6672	0
R236ea	1,1,1,2,3,3-Hexafluoropropane	279.322	412.44	3.42	0.9686	1.7817	−0.7588	0
R236fa	1,1,1,3,3,3-Hexafluoropropane	271.66	398.07	3.2	0.9612	1.0095	1.2126	0
R245ca	1,1,2,2,3-Pentafluoropropane	298.412	447.57	3.9407	1.0738	0.7334	1.6227	0
R245fa	1,1,1,3,3-Pentafluoropropane	288.198	427.01	3.651	0.9972	0.7270	2.2701	0
R1234yf	2,3,3,3-Tetrafluoroprop-1-ene	243.665	367.85	3.3822	0.9788	0.9605	1.1780	0
R1234ze(E)	trans-1,3,3,3-Tetrafluoropropene	254.177	382.513	3.6349	1.0111	0.1065	7.0036	−0.9997
R1243zf	3,3,3-Trifluoroprop-1-ene	247.726	376.93	3.5179	1.0356	1.2500	0	0

for some newly-emerging low-GWP fluids are insufficient to cover a wide range of residual entropy for the development of RES correlation. Therefore, we are prompted to take advantage of the common features of HFCs/HFOs by collapsing data of all investigated fluids to a single RES curve, which takes the formulation of

$$\ln \lambda^* = B_1 \cdot \left(\frac{s^{res}}{\zeta R}\right)^{\frac{1}{3}} + B_2 \cdot \left(\frac{s^{res}}{\zeta R}\right)^{\frac{2}{3}} + B_3 \cdot \left(\frac{s^{res}}{\zeta R}\right) + B_5 \cdot \left(\frac{s^{res}}{\zeta R}\right)^{\frac{5}{3}} + B_{-1} \cdot \left[\exp\left(-B_0 \cdot \frac{s^{res}}{\zeta R}\right) - 1\right] \quad (9)$$

where B_i denotes the coefficients, of which the values are given in Table 3, and ζ is the rescaling parameter to benchmark the residual entropy of the fluids against the single RES curve. The coefficients of the RES curve, B_i, are fitted with R134a at first because R134a has the most extensive experimental data which cover a wide thermodynamic state region. From this perspective, R134a is selected as a reference to capture the trend. Thus, the value of the rescaling parameter ζ is set to unity for R134a. As shown in Fig. 3 (a), the correlation curve is in good agreement with the data of R134a, while the data of the other 14 fluids deviate positively or negatively from the curve. For each of the fluids except R134a, ζ is obtained by minimizing the summation of the squared relative deviation of the calculated value of Eq. (9) from the experimental data. Fig. 3 (b) shows the reduced thermal conductivity data against the rescaled residual entropy (s^{res} / ζ). With the introduction of ζ, the data for all the investigated fluids are closely mapped onto the single RES curve fitted with R134a. Table 1 lists the values of ζ of all the investigated fluids. The approach using the single RES curves to capture the common features of the investigated fluids was also applied in our previous work [8,9] and Refs. [107, 108]. In this approach, the RES model not only represents all the investigated fluids and their mixtures by capturing the common trend in λ^*-s^{res}, but also makes possible future extensions of the model to other, newer compounds of the same family.

2.4. Mixture modeling

Assuming the mixture thermal conductivity to follow the common trend in λ^*-(s^{res} / ζ), the RES curve, Eq. (9), is extended to the binary mixtures of the investigated fluids. The extension is related to three aspects: the CPA equation of state, reference thermal conductivity, and the rescaling parameter ζ.

The CPA equation of state can be readily extended to the binary mixtures using the van der Waals mixing rules for the SRK parameters and the Elliot combining rule [109] for the association strength between molecules of different components. The reference thermal conductivity in Eq. (6) can be extended to mixtures with the dilute gas mixture thermal conductivity predicted by the Hirschfelder-Eucken expression [110]. Readers can refer to the supplementary materials for the mixing/combining rules of the CPA equation of state and the dilute gas transport property models for the mixtures derived by the kinetic theory.

The arithmetic mean mixing rule of the rescaling parameter ζ, i.e., $\zeta = x_1\zeta_1 + x_2\zeta_2$, has been successfully applied in the recent works [25,26]. From this perspective, the mixture model is predictive. The experimental data are needed for the model validation. Table 4 shows an overview of the experimental data for binary mixtures. For detailed information on the experimental data, please refer to Table S7 in the supplementary materials.

Fig. 4 (a) and (b) shows the data of R125 + R134a and R32 + R125 as examples in reduced thermal conductivity against residual entropy. For most of the investigated binary mixtures, such as R125 + R134a, the data can be readily mapped onto the RES curve, following the mixture model. However, the model is not so applicable for some of the mixtures, especially R32 + R125 and R32 + R134a. As shown in

Table 2
Experimental data and relative deviations of pure fluids.

Fluid	Experimental data			Deviation / %	
	T / K	p / MPa	N	RMS [a]	δ_{max} [b]
R23 [c]	192 to 455	0.1 to 39.3	320	3.3	9.8
R32 [d]	223 to 466	0.1 to 50	999	2.8	14.5
R125 [e]	225 to 513	0.04 to 36	1673	2.3	8.8
R134a [f]	248 to 533	0 to 40	6271	2.5	11
R143a [g]	233 to 499	0.1 to 37.1	539	2.1	7.7
R152a [h]	250 to 510	0.03 to 45	1734	3.5	13.3
R161 [i]	236 to 381	0.1 to 5.2	361	2.1	7.3
R227ea [j]	282 to 344	0.04 to 2.9	291	1.5	5
R236ea [k]	281 to 334	0.05 to 0.5	202	1.6	4.5
R236fa [l]	273 to 375	0.03 to 30	256	2.1	5.2
R245ca [m]	298 to 393	0.03 to 0.3	131	2.2	5.8
R245fa [n]	290 to 416	0.1 to 35.5	555	2.9	10.4
R1234yf [o]	244 to 344	0.1 to 21.7	744	1.0	5.1
R1234ze(E) [p]	255 to 402	0.05 to 23.3	1102	1.7	7.7
R1243zf [q]	314 to 406	0.9 to 6.1	35	5.7	14.5
Overall	192 to 533	0 to 50	15,213	2.5	14.5

[a] RMS $= \sqrt{\sum \left[\left(\lambda_{exp} - \lambda_{cal}\right)/\lambda_{cal}\right]^2/N}$.
[b] Relative deviation $\delta = (\lambda_{cal} - \lambda_{exp})/\lambda_{exp}$.
[c] Reference: [33–39].
[d] Reference: [40–50].
[e] Reference: [40–42, 44, 46–48, 50–60].
[f] Reference: [41, 43, 50–52, 54, 57, 58, 61–79].
[g] Reference: [46, 80, 81].
[h] Reference: [37, 39, 41, 66, 74, 82–93].
[i] Reference: [94].
[j] Reference: [95, 96].
[k] Reference: [95].
[l] Reference: [95, 97].
[m] Reference: [95, 98].
[n] Reference: [98–103].
[o] Reference: [104].
[p] Reference: [104, 105].
[q] Reference: [106].

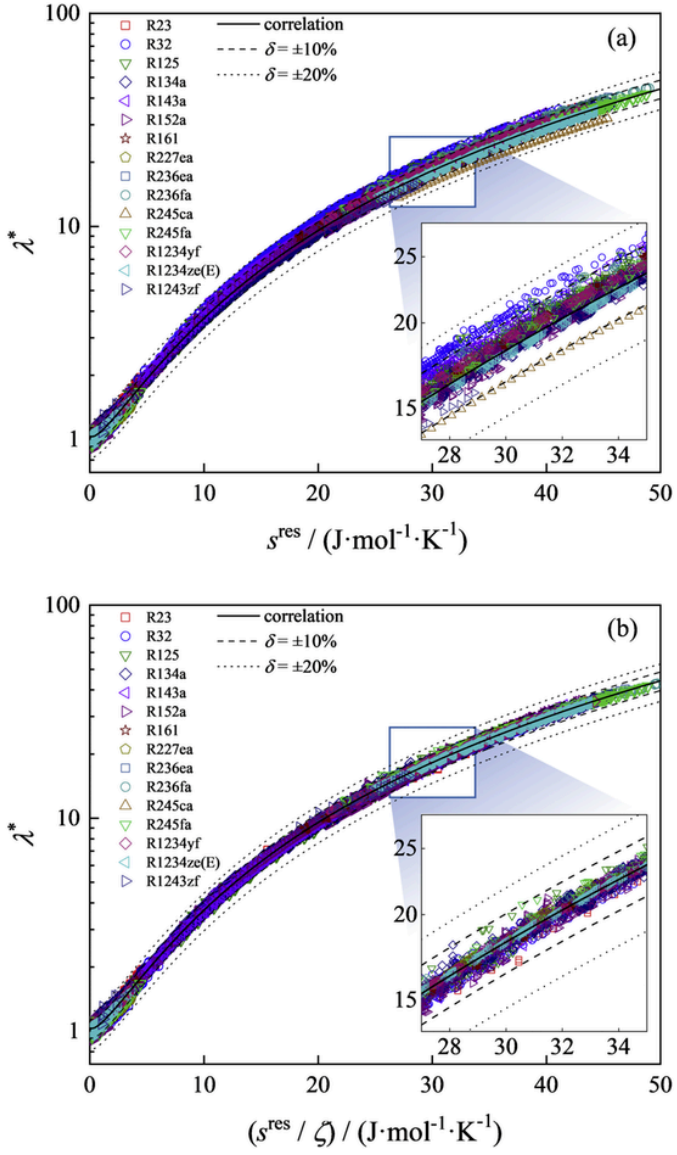

Fig. 3. Reduced thermal conductivity for the pure fluids as a function of (a) residual entropy and (b) rescaled residual entropy.

Table 3
Coefficients of Eq. (9).

i	B_i
1	0.4853527
2	−2.380075
3	1.799938
5	−0.1274701
−1	−2.514361
0	0.7490895

Fig. 4 (b), the data points of the mixture R32 + R125 fall below the points of pure R32 and R125 at the same residual entropy. Thus, the binary mixture R32 + R125 would have a larger ζ than both of its pure components, which deviates significantly from any type of average mixing rule, including arithmetic and geometric. Therefore, we turn to investigate the reference thermal conductivity.

Table 4
Experimental data and deviations of the binary mixtures.

Mixture	Experimental data [a]				Deviation / %	
	x_1	T / K	p / MPa	N	RMS [a]	δ_{max} [b]
R32 + R125 [c]	0.19 to 0.88	233 to 428	0.1 to 30	453	3.4	8.5
R32 + R134a [d]	0.3 to 0.85	248 to 385	0.1 to 30	1425	4.5	9.4
R32 + R1234yf [e]	0.25 to 0.75	264 to 395	0.9 to 4	36	4.9	13.5
R32 + R1243zf [e]	0.25 to 0.75	264 to 395	1 to 4	37	4.9	13.3
R125 + R134a [f]	0.19 to 0.79	248 to 387	0.1 to 20	1160	4.1	8.4
R125 + R143a [g]	0.41	255 to 372	0.1 to 3.8	162	4.9	13.1
R125 + R152a [h]	0.5	274 to 394	1 to 3.1	11	4.5	7.6
R125 + R1234yf [h]	0.5	260 to 394	1.1 to 3.1	12	3.5	6.5
R125 + R1234ze(E) [h]	0.5	263 to 395	1 to 3.1	12	3.0	4.3
R134a + R1234yf [i]	0.5	255 to 385	1 to 3	12	5.3	11
R134a + R1234ze(E) [h]	0.5	275 to 404	0.9 to 3.1	12	6.4	10.5
R143a + R1234yf [h]	0.5	265 to 394	1.1 to 3.1	12	2.3	5.4
R143a + R1234ze(E) [h]	0.5	265 to 404	0.9 to 3	12	4.2	9.4
R1234yf + R1234ze(E) [h]	0.5	275 to 414	0.9 to 3	12	3.4	6.6
Overall	–	**233 to 428**	**0.1 to 30**	**3368**	**4.3**	**13.5**

[a] RMS $= \sqrt{\sum \left[\left(\lambda_{exp} - \lambda_{cal}\right)/\lambda_{cal}\right]^2/N}$.
[b] Relative deviation $\delta = (\lambda_{cal} - \lambda_{exp})/\lambda_{exp}$.
[c] References: [44, 47, 50, 111–114].
[d] References: [43, 111, 114, 115].
[e] References: [106]
[f] References: [58, 114, 115].
[g] References: [112, 116].
[h] References: [117].
[i] References: [114].

Fig. 5 compares λ^{ref} calculated by Eq. (6) with the experimental value. For R125 + R134a, the reference thermal conductivity calculated using Eq. (6) is almost a linear function of the mole fraction and follows the experimental data points, while for R32 + R125, the reference thermal conductivity is a concave function of the mole fraction and expected to be more concave. Therefore, we revise the formulation of reference thermal conductivity,

$$\lambda^{ref}\left(T, x_1, s^{res}\right) = \eta^{o}\left(T, x_1\right) \cdot \frac{15R}{4M\left(x_1\right)} \cdot \left(1 - \alpha\left(s^{res}\right)\right) + \lambda^{o}\left(T, x_1\right) \cdot \alpha\left(s^{res}\right) \tag{10}$$

where the dilute gas viscosity η^o and thermal conductivity λ^o for binary mixtures are obtained by the kinetic theory, and M is the molar weighted arithmetic mean of the mole fraction. Here, the model using Eq. (6) is denoted as the RES-CPA model; that using Eq. (10) is denoted as the r-RES-CPA model. For the pure fluids, the r-RES-CPA model reduces to the RES-CPA model, as x_1 approaches to 1 or 0. For the mixtures in the dense region, the reference thermal conductivity of the RES-CPA model approximately equals the translational term of the dilute gas thermal conductivity, while the reference thermal conductivity of r-RES-CPA is proportional to the dilute gas viscosity. For R125 + R134a, both models are equally good. For R32 + R125, the r-RES-CPA captures the more concave trend of experimental data and is more accurate, as shown in Fig. 4 (c) and Fig. 5.

In brief, the mixture thermal conductivity follows the common trend in λ^*-(s^{res} / ζ) represented by Eq. (9). The reduced thermal conductivity, λ^*, is derived from Eq. (10). The residual entropy, s^{res}, is derived from the CPA equation of state [7]. The rescaling parameter, ζ, is obtained by the arithmetic mean mixing rule. The mixing/combining rules of the dilute gas model in Eq. (10) and of the CPA equation of state are provided in the supplementary materials.

3. Results and discussion

3.1. Range of applicability

The range of applicability of RES law depends on the strength of the correlation between virial and potential energy. The strength is indicated by the correlation coefficient [118]. Bell et al. [21] analyzed the simulation results of Costigliola et al. [119] on the Lennard-Jones fluid: the correlation coefficient in the liquid and supercritical regions is close to unity, indicating a strong correlation and thus a good scaling performance; as the temperature and density decrease, the correlation coefficient also decreases, indicating the possibility of the deviation of reduced thermal conductivity from the univariate dependence on residual entropy. The model's range of applicability also depends on the CPA equation of state, which yields the input parameter of the RES model, i.e., residual entropy. The parameters of CPA equation of state were fitted to the experimental data in the subcritical region between T_{nb} (normal boiling point) and $0.9T_{cr}$ (critical temperature) and up to $5p_{cr}$ (critical pressure) in our previous work [7]. Near the critical point, thermodynamic properties are extremely sensitive to the thermodynamic state. The models proposed by Kiselev et al. [120–122] and White et al. [123,124] are promising to capture these features. With the support of an accurate thermodynamic model, a critical enhancement term [125,126] can be included in the RES model to represent the divergence of thermal conductivity near the critical point, which was adopted in the recent RES models for Lennard-Jones fluid [20,21]. However, regression of the model parameters that are related to the near-critical region requires accurate thermodynamic and

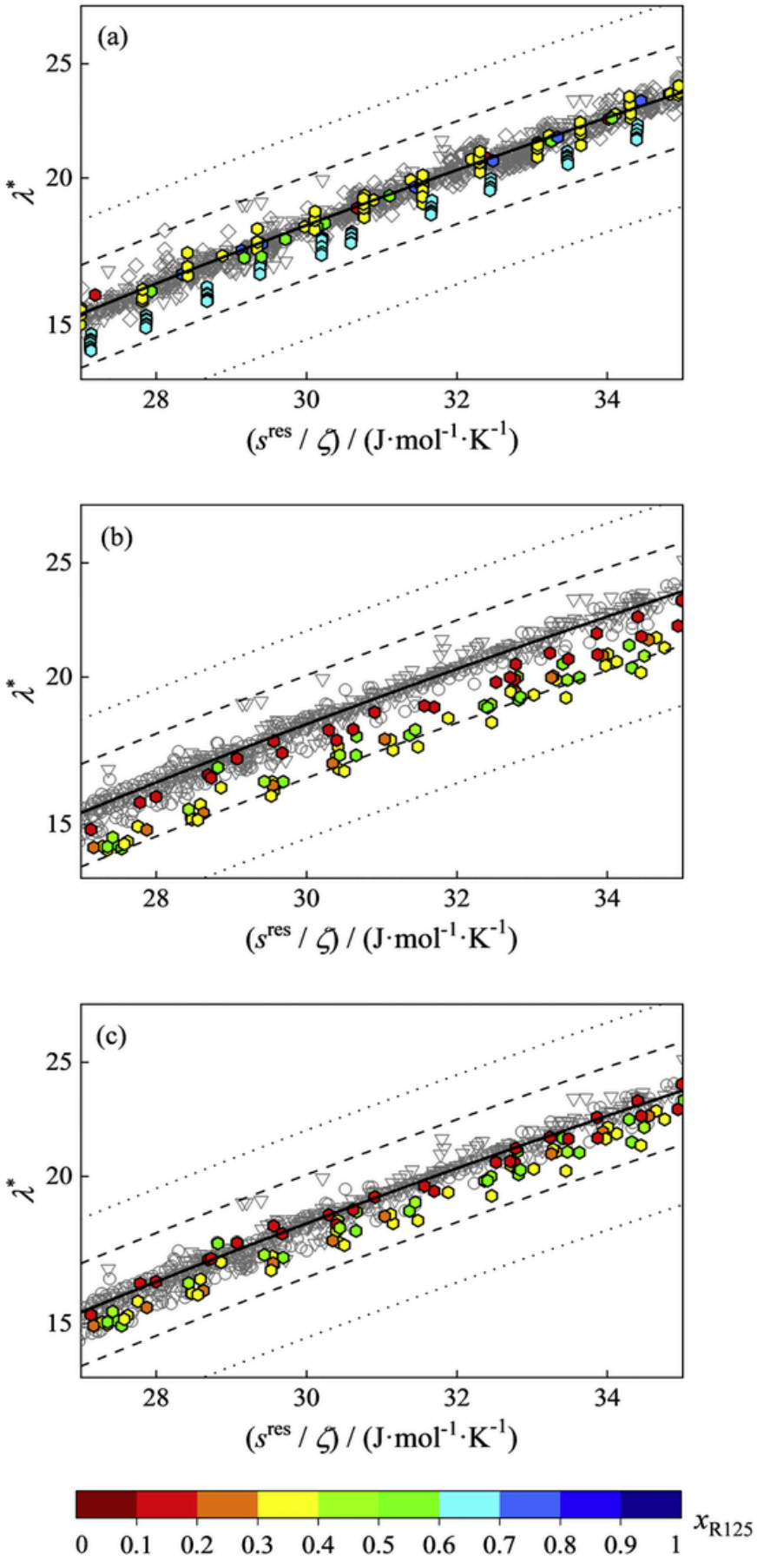
(a)
(b)
(c)
λ*
25
20
15
28
30
32
34
(s^res / ζ) / (J·mol^-1·K^-1)
0
0.1
0.2
0.3
0.4
0.5
0.6
0.7
0.8
0.9
1
x_R125

Fig. 4.

transport property data, which are not available for most of the investigated fluids in the present work.

According to the practice and the fitting range of the CPA equation of state, the lower limit of the temperature and upper limit of the pressure are T_{nb} and $10p_{cr}$, respectively. The near-critical region is also excluded from the range of applicability.

Fig. 6 shows the relative deviation of the model from the experimental data of all the investigated pure fluids. To visualize the applicability, the data near the critical point, which are obviously beyond the range of applicability of the model, are included. The relative deviation is defined as

$$\delta = \left(\lambda_{cal} - \lambda_{exp}\right) / \lambda_{exp} \tag{11}$$

The deviation of the model is generally smaller than 5% in the liquid region and in which the temperature is far higher than T_{cr}. No more than 2% of the data have large deviations of 10% to 15%. These data are mainly distributed in the gas phase. The data in the supercritical region are also included in the modeling due to their low deviations from the model, and these data make the scaling curves in Fig. 3 continuous instead of being separated into two clusters of the gas and liquid region. In the vicinity of the critical point, the deviation is larger than 15%, mainly due to the critical enhancement: a slight change in temperature or pressure may cause a significant change in thermal conductivity. Therefore, the model deviates from the real characteristics in the region near the critical point, or to be more specific, the region with the temperature between $0.95T_{cr}$ and $1.1T_{cr}$ and the pressure between $0.7p_{cr}$ and $1.5p_{cr}$ as shown in Fig. 6. In the following validation procedure, the data within the above range will be removed.

In summary, the RES-CPA model is applicable in wide ranges of temperature and pressure including the gas, liquid, and supercritical regions, except for the region in the vicinity of critical point ($0.95T_{cr} < T < 1.1T_{cr}$ and $0.7p_{cr} < p < 1.5p_{cr}$) with a simple formulation of a univariate function of residual entropy.

3.2. Pure fluids

The RES-CPA model is based on the correlation for R134a. Therefore, the correlation is the first to be validated by the comparison to the experimental data of R134a. Perkins et al. [78] contributed the major portion of the experimental data, of which the reliability is corroborated by the data from other sources and the RES-CPA model. 80% of the R134a data agree with the model within 3%, and only 5% of the data with deviations larger than 5%. Fig. 7 shows the relative deviation of the model from experimental data as a function of temperature and pressure. The deviation does not show any obvious trend with the increase of either temperature or pressure.

The RES curve is fitted and validated with the experimental data of R134a covering wide ranges of temperature and pressure. It captures the trend and can be extended to the fluids in the same family of which the experimental data are scarce or unavailable. The results for the other 14 fluids are compared to the experimental data to validate Eq. (9). Table 2 lists the root mean square (RMS) and maximum (max) deviations of the model for each pure fluid. Fig. 8 shows the data distribution and deviation histogram. With a single adjustable parameter ζ introduced, the model shows comparable performance to that for R134a: 82% of data points are accurately reproduced within 3% deviation; the deviation shows no obvious trend with the increase of temperature or pressure. Therefore, taking advantage of the common features of the compounds, it is not necessary to fit the model parameters separately for each fluid. Rescaling the residual entropy and fitting the single RES curve is a feasible method to predict the thermal conductivity of the fluids in the same family.

3.3. Binary mixtures

The mixture model is extended from the 'universal' RES curve without fitting the mixture data. It accounts for the interaction of the two components in the binary mixture with the aid of the mixing/combining rules in the CPA equation of state and dilute gas transport property model. Available thermal conductivity data of binary mixtures are collected for the validation of the model.

Fig. 9 shows the reduced thermal conductivity of the binary mixtures along with the pure fluids as a function of residual entropy. The mixture curves collapse to the reference (pure fluid) curve. The vast majority of data are distributed within 10%.

Table 4 lists the maximum and average relative deviations of the model with experimental data for each binary mixture. Fig. 10 shows the data distribution and deviation histogram for each binary mixture. With no additional fitted mixture-specific parameter, the model shows acceptable results for the binary mixture: the calculated results mostly show a slight positive deviation from the experimental data while 73% of the data are reproduced within 5%; the deviation shows no obvious trend with the increase of temperature, pressure or molar fraction.

The results of the RES-CPA and r-RES-CPA using different reference thermal conductivity are also compared in Fig. 10. For the mixtures with extensive data such as R32 + R125 and R32 + R134a, the RES-CPA model shows larger positive deviations than r-RES-CPA. The introduction of mixture-specific parameters is likely to bring the relative deviation closer to a normal distribution centered at zero. However, due to the limited sources and ranges of experimental data, the development of a predictive model is the top priority. Additional data will be appreciated for the development of empirical as well as semi-theoretical models, including the further improvement of the formulation of the reference thermal conductivity obtained by induction in this work.

3.4. Rescaling parameters

For the monatomic fluids, it was verified that the transport properties can collapse onto a single RES curve with no substance-specific parameter using the simulation results of Lennard-Jones fluid [20,127] and experimental data of noble

Reduced thermal conductivity of the RES-CPA model for (a) R125 + R134a and (b) R32 + R125 and the revised reduced thermal conductivity of the r-RES-CPA model for (c) R32 + R125 as a function of residual entropy. (hexagon dots with color filled: mixtures; triangle dots: R125; diamond dots: R134a; circle dots: R32; solid curve: the RES correlation, Eq. (9); dashed curve: $\delta = \pm 10\%$; dotted curve: $\delta = \pm 20\%$).

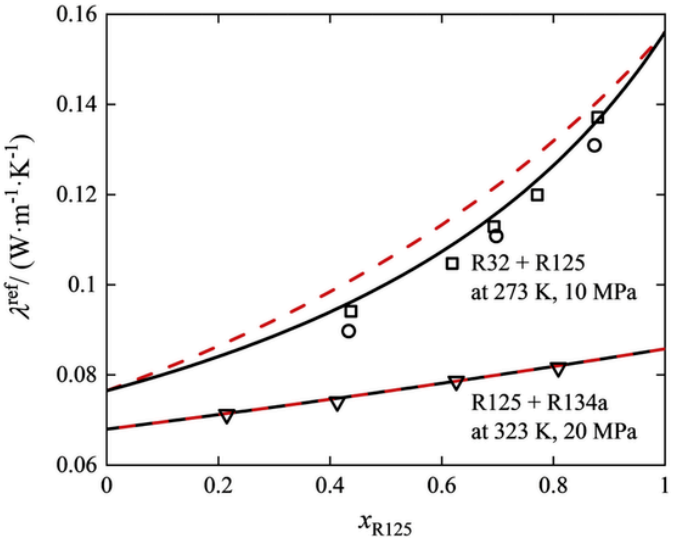

Fig. 5. Reference thermal conductivity of the binary mixtures R125 + R134a at 323 K, 20 MPa, and R32 + R125 at 273 K, 10 MPa in the RES-CPA model (red dashed curve), r-RES-CPA model (black solid curve), and the experimental data (triangle dots: Jeong (1999) [58]; square dots: Ro (1997) [47]; circle dots: Gao (1999) [111]).

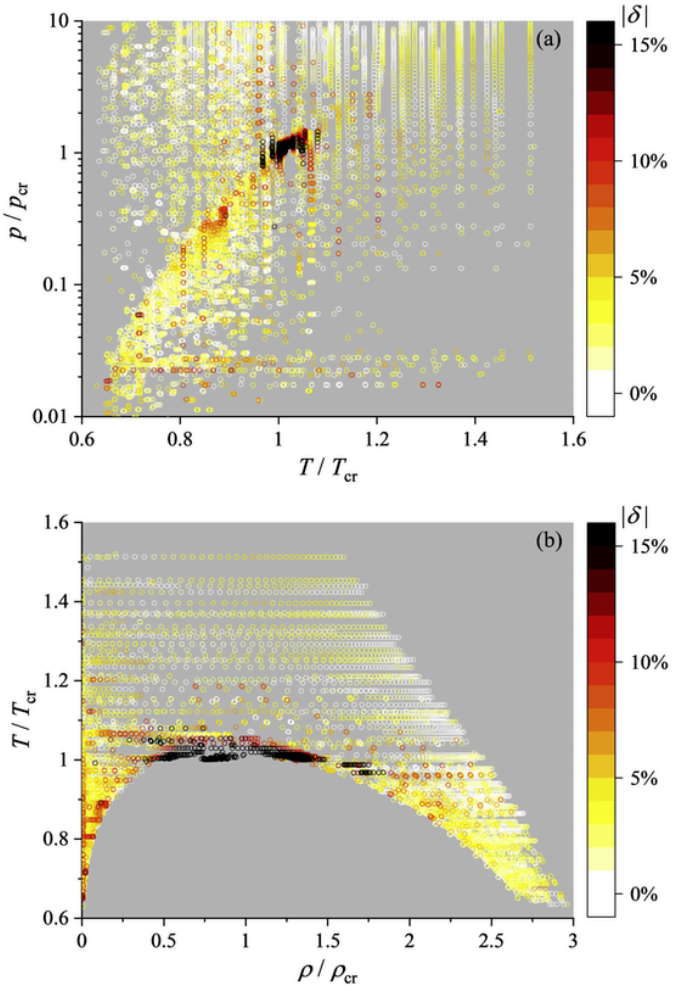

Fig. 6. Relative deviation in the reduced ranges of temperature, pressure, and density relative to their values at the critical point.

gases [128]. For the Lennard-Jones chain fluids [20,127] and normal alkanes [107], the reduced transport properties show the univariate dependence on residual entropy. The slope of scaling curves in the dense region varies monotonously with the chain length. For the HFCs/HFOs, the curves also scatter in the dense region. Therefore, in the RES-CPA model, the fluid-specific rescaling parameter, ζ for the thermal conductivity, and ξ for the viscosity in our previous work [8,9], are proposed to rescale the data of all investigated pure fluids into a single RES curve of the investigated fluids. It is not difficult to infer that the rescaling parameter is related to the molecular structure. However, it is no easy task to reveal the relationship between the rescaling parameter and molecular structure or to propose a pure predictive approach to obtain ξ or ζ with some basic parameters regarding such a limited number of fluids with complex molecular structures including branches, double bonds, association, etc. Therefore, in both studies, ξ or ζ is obtained with an empirical approach by minimizing $\sum\delta_i^2$. In both studies, the values of the rescaling parameters for the reference fluid, R134a, are set to unity. The values larger than unity are used to correct the positive deviation from the reference RES curve and the values smaller than unity to correct the negative deviation. The parameters ξ and ζ do not show obvious correlation. Also, either of them does not show obvious correlation with other basic parameters, e.g., acentric factor, dipole moment, critical and Lennard-Jones parameters. In general, the introduction of ξ and ζ as the only adjustable parameter is an advantageous approach to develop the RES model for the fluids belonging to the same family. Its relationship with molecular structure remains to be explored.

4. Conclusions

In this work, we model the thermal conductivity of HFCs, HFOs, and their binary mixtures using the RES approach and CPA equation of state. In wide ranges of temperature and pressure except for the near-critical region, the dependence of the thermal conductivity on the thermodynamic state is reduced to a univariate function of residual entropy, i.e., the data on the thermodynamic phase diagram are mapped onto a single coordinate of residual entropy. Thus, the lack or uneven distribution of the data can be readily overcome.

Taking advantage of the common features of molecular structure and intermolecular interaction of HFCs/HFOs, our previous procedure for the viscosity, i.e., correlating the RES curve using the data of R134a and then fitting the single rescaling parameter for each pure fluid, is applied for the thermal conductivity successfully and clarified to be advantageous to develop the RES model for the homogeneous fluids. A new reference thermal conductivity formulation is proposed to obtain the univariate function relationship and improve the prediction accuracy for mixtures. For the investigated pure fluids, the overall RMS deviations of the RES-CPA model is 2.5%, and the maximum deviation from experimental data is 14.5%. The 14 pure fluids, with only one adjustable parameter for each, show similarly accurate results to the reference fluid, R134a. For the 14 binary mixtures, with the newly proposed reference thermal conductivity, the overall RMS and maximum deviations are 4.3% and 13.5%, respectively.

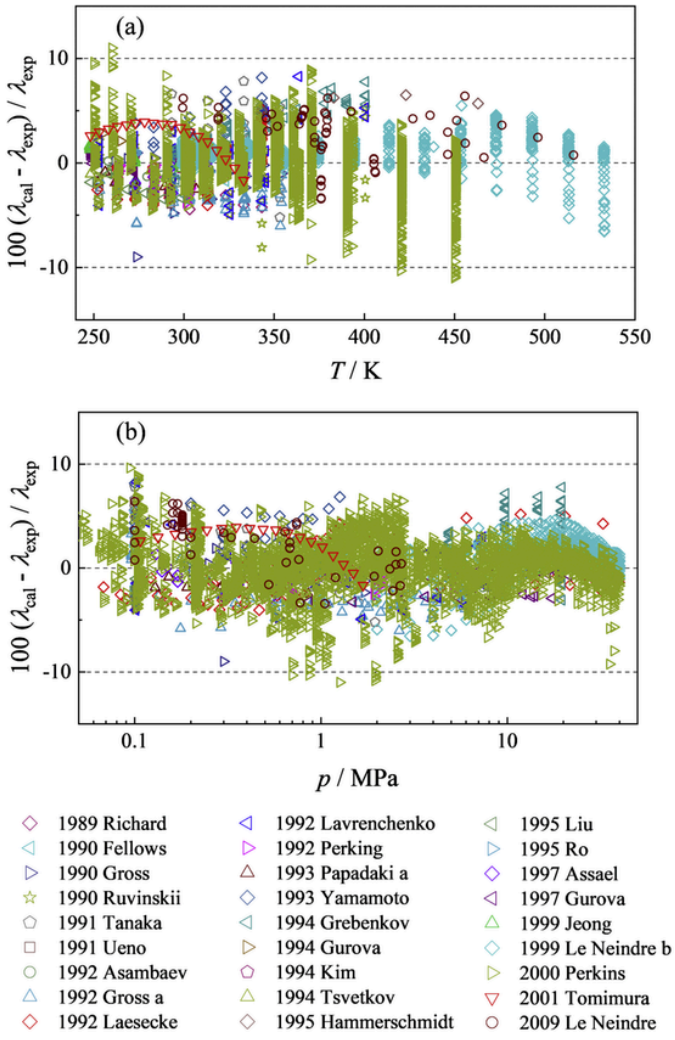

Fig. 7. Relative deviation of RES-CPA model from the experimental data of R134a as a function of (a) temperature and (b) pressure.

Author statement

Hangtao Liu: Conceptualization, Methodology, Data Curation, Software, Validation, Investigation, Writing-Original Draft, Visualization.

Fufang Yang: Conceptualization, Software, Writing-Review & Editing.

Xiaoxian Yang: Conceptualization, Data Curation, Writing-Review & Editing.

Zhen Yang: Conceptualization, Resources, Writing-Review & Editing, Supervision.

Yuanyuan Duan: Conceptualization, Resources, Writing-Review & Editing, Supervision, Funding acquistion.

Uncited references

[34–36,38,45,49,51,53,55,56,59,62–65,67–73,75–77,83–92,99–102,113]

Declaration of Competing Interest

The authors declare that they have no known competing financial interests or personal relationships that could have appeared to influence the work reported in this paper.

Acknowledgments

This work was supported by the National Natural Science Foundation of China [Grant No. 51736005].

Appendix A. Supplementary material

The supplementary material file includes the formulas and parameters of the residual entropy and dilute gas transport properties, and detailed information on the literature data sources for each fluid.

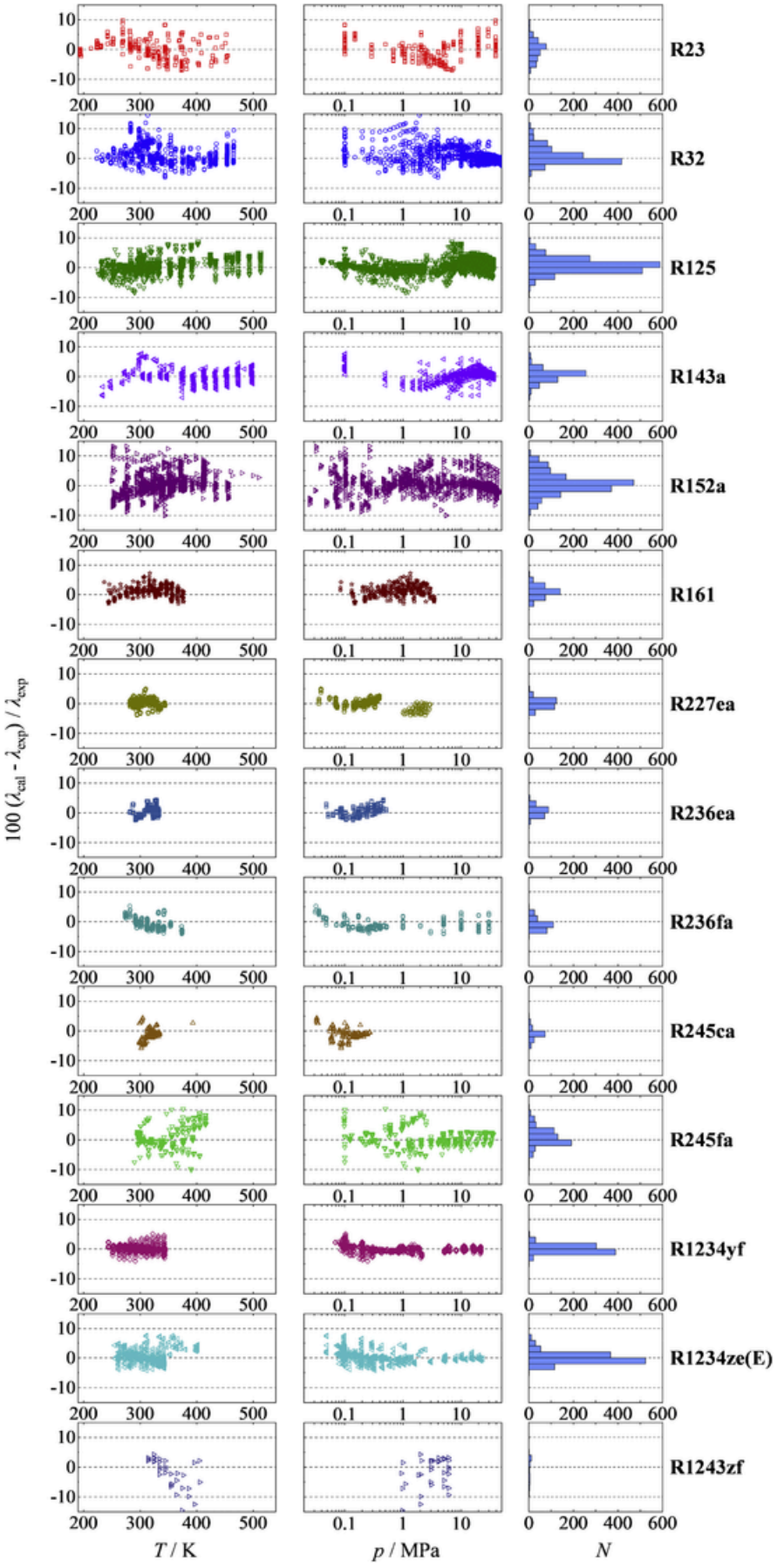
100 (λcal - λexp) / λexp
T / K
p / MPa
N
R23
R32
R125
R143a
R152a
R161
R227ea
R236ea
R236fa
R245ca
R245fa
R1234yf
R1234ze(E)
R1243zf

Fig. 8.

Relative deviation of RES-CPA model from the experimental data of other pure HFCs/HFOs as a function of temperature, pressure and the histograms of the deviation.

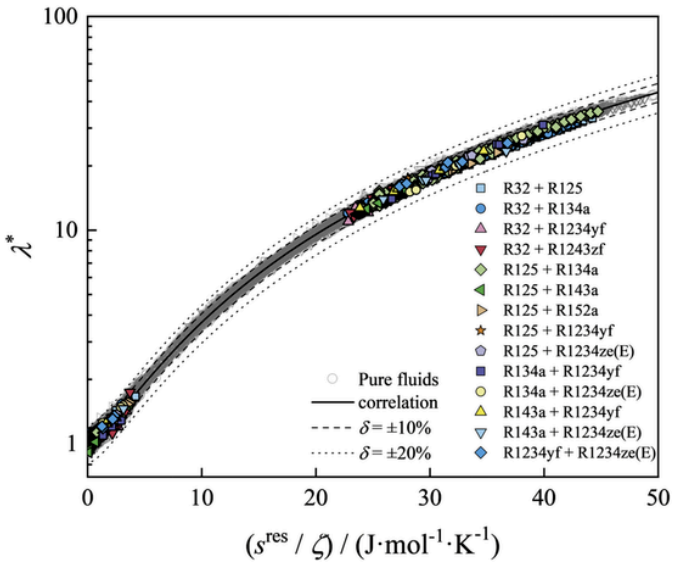

Fig. 9. Reduced thermal conductivity for pure fluids and binary mixtures as a function of rescaled residual entropy.

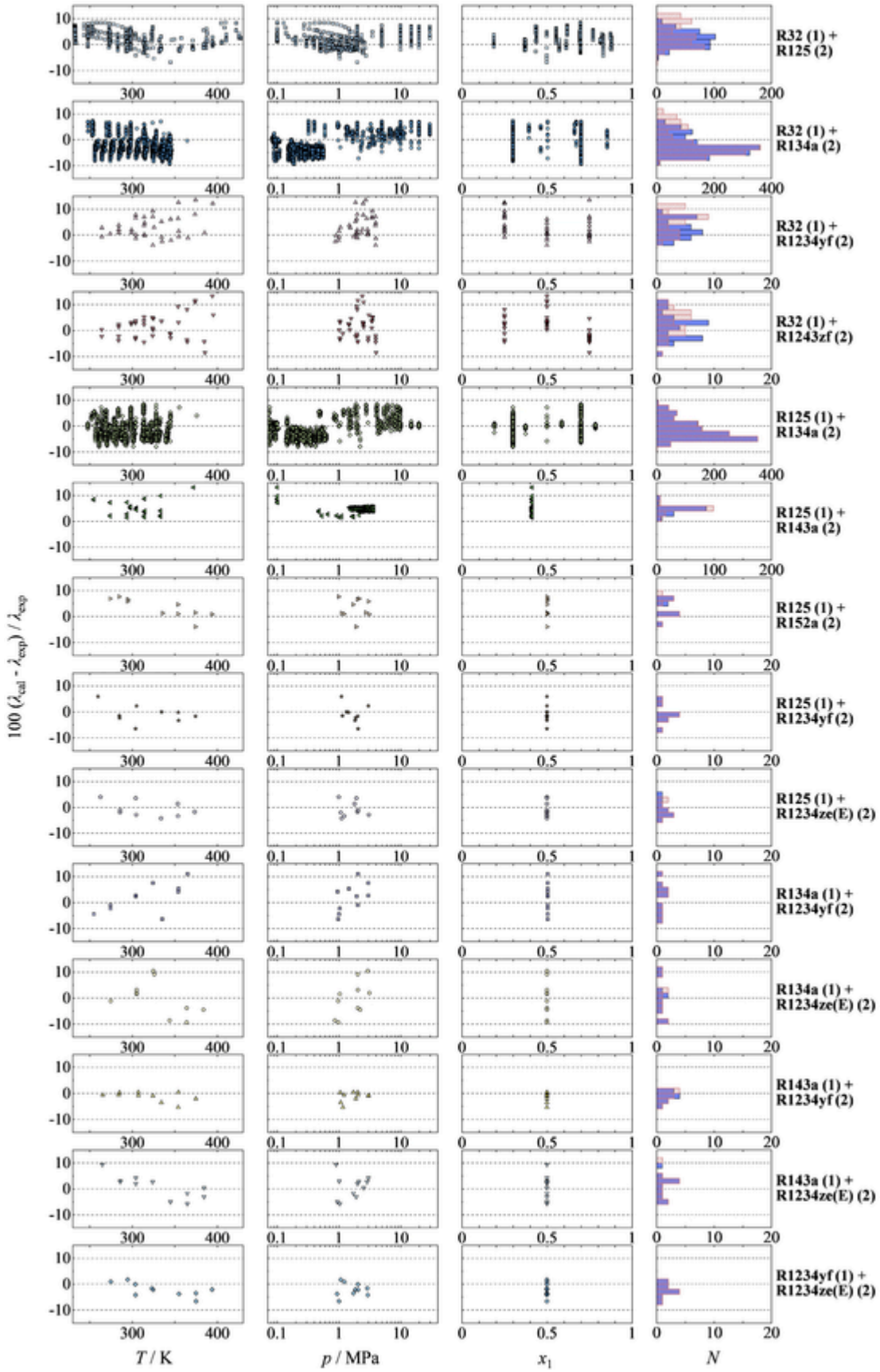
100 (λcal - λexp) / λexp
T / K
p / MPa
x1
N
R32 (1) + R125 (2)
R32 (1) + R134a (2)
R32 (1) + R1234yf (2)
R32 (1) + R1243zf (2)
R125 (1) + R134a (2)
R125 (1) + R143a (2)
R125 (1) + R152a (2)
R125 (1) + R1234yf (2)
R125 (1) + R1234ze(E) (2)
R134a (1) + R1234yf (2)
R134a (1) + R1234ze(E) (2)
R143a (1) + R1234yf (2)
R143a (1) + R1234ze(E) (2)
R1234yf (1) + R1234ze(E) (2)

Fig. 10. Relative deviation of the r-RES-CPA model from the experimental data of HFC/HFO binary mixtures as a function of temperature, pressure, and mole fraction, and the histograms of the deviation of the RES-CPA (red slash filled) and r-RES-CPA (blue solid filled) model with different reference thermal conductivity.

References

[1] M.O. McLinden, M.L. Huber, J. Chem. Eng. Data 65 (2020) 4176–4193, doi:10.1021/acs.jced.0c00338.
[2] J. Li, Q. Liu, Z. Ge, Y. Duan, Z. Yang, Energy Convers. Manag. 149 (2017) 140–154, doi:10.1016/j.enconman.2017.06.060.
[3] J. Li, Z. Ge, Y. Duan, Z. Yang, Q. Liu, Appl. Energy 217 (2018) 409–421, doi:10.1016/j.apenergy.2018.02.096.
[4] S. Hu, J. Li, F. Yang, Z. Yang, Y. Duan, Energy 203 (2020) 117848, doi:10.1016/j.energy.2020.117848.
[5] F. Yang, F. Yang, Q. Chu, Q. Liu, Z. Yang, Y. Duan, Energy Convers. Manag. 217 (2020) 113011, doi:10.1016/j.enconman.2020.113011.
[6] M.O. McLinden, J.S. Brown, R. Brignoli, A.F. Kazakov, P.A. Domanski, Nat. Commun. 8 (2017) 14476, doi:10.1038/ncomms14476.
[7] F. Yang, Q. Chu, Q. Liu, Y. Duan, Z. Yang, Chem. Eng. Sci. 209 (2019) 115182, doi:10.1016/j.ces.2019.115182.
[8] H. Liu, F. Yang, Z. Yang, Y. Duan, J. Mol. Liq. 308 (2020) 113027, doi:10.1016/j.molliq.2020.113027.
[9] X. Yang, H. Liu, S.H. Chen, D. Kim, F. Yang, A. Arami-Niya, Y. Duan, Int. J. Refrigeration (2020) JIJR4974, In press.
[10] T.H. Chung, M. Ajlan, L.L. Lee, K.E. Starling, Ind. Eng. Chem. Res. 27 (1988) 671–679, doi:10.1021/ie00076a024.
[11] M. Bugel, G. Galliero, Chem. Phys. 352 (2008) 249–257, doi:10.1016/j.chemphys.2008.06.013.
[12] M.O. McLinden, S.A. Klein, R.A. Perkins, Int. J. Refrig. 23 (2000) 43–63, doi:10.1016/s0140-7007(99)00024-9.
[13] M.L. Huber, NIST Interagency/Internal Report, NIST, Boulder, Colorado, 2018, doi:10.6028/nist.Ir.8209.
[14] E.W. Lemmon, I.H. Bell, M.L. Huber, M.O. McLinden, REFPROP Documentation Release 10.0 Boulder, Colorado 2018.
[15] J.H. Dymond, Int. J. Thermophys. 18 (1997) 303–312, doi:10.1007/bf02575162.
[16] X. Gao, M.J. Assael, Y. Nagasaka, A. Nagashima, Int. J. Thermophys. 21 (2000) 23–34, doi:10.1023/a:1006696518938.
[17] X. Liu, C. Wang, T. Lan, M. He, Y. Zhang, ACS Sustain. Chem. Eng. 8 (2020) 6022–6032, doi:10.1021/acssuschemeng.0c00801.
[18] Y. Rosenfeld, Phys. Rev. A 15 (1977) 2545–2549, doi:10.1103/PhysRevA.15.2545.
[19] Y. Rosenfeld, J. Phys. Condens. Matter 11 (1999) 5415–5427, doi:10.1088/0953-8984/11/28/303.
[20] G. Galliero, C. Boned, Phys. Rev. E Stat. Nonlinear Soft Matter Phys. 80 (2009) 061202, doi:10.1103/PhysRevE.80.061202.
[21] I.H. Bell, R. Messerly, M. Thol, L. Costigliola, J.C. Dyre, J. Phys. Chem. B 123 (2019) 6345–6363, doi:10.1021/acs.jpcb.9b05808.
[22] M. Hopp, J. Gross, Ind. Eng. Chem. Res. 56 (2017) 4527–4538, doi:10.1021/acs.iecr.6b04289.
[23] W.A. Fouad, L.F. Vega, J. Supercrit. Fluids 131 (2018) 106–116, doi:10.1016/j.supflu.2017.09.006.
[24] M. Hopp, J. Gross, Ind. Eng. Chem. Res. 58 (2019) 20441–20449, doi:10.1021/acs.iecr.9b04289.
[25] H.B. Rokni, J.D. Moore, A. Gupta, M.A. McHugh, R.R. Mallepally, M. Gavaises, Fuel 245 (2019) 594–604, doi:10.1016/j.fuel.2019.02.044.
[26] W.A. Fouad, J. Chem. Eng. Data (2020), doi:10.1021/acs.jced.0c00682.
[27] M.J. Assael, K.D. Antoniadis, W.A. Wakeham, Int. J. Thermophys. 31 (2010) 1051–1072, doi:10.1007/s10765-010-0814-9.
[28] G.M. Kontogeorgis, I.V. Yakoumis, H. Meijer, E. Hendriks, T. Moorwood, Fluid Phase Equilib. 158–160 (1999) 201–209, doi:10.1016/S0378-3812(99)00060-6.
[29] G.M. Kontogeorgis, I.G. Economou, J. Supercrit. Fluids 55 (2010) 421–437, doi:10.1016/j.supflu.2010.10.023.
[30] F. Yang, Q. Liu, Y. Duan, Z. Yang, Chem. Eng. Sci. 192 (2018) 565–575, doi:10.1016/j.ces.2018.08.014.
[31] P.D. Neufeld, A.R. Janzen, R.A. Aziz, J. Chem. Phys. 57 (1972) 1100–1102, doi:10.1063/1.1678363.
[32] E. Lemmon, I.H. Bell, M. Huber, M. McLinden, NIST Standard Reference Database 23: Reference Fluid Thermodynamic and Transport Properties-REFPROP, Version 10.0, NIST, Boulder, Colorado, 2018.
[33] V.Z. Geller, S.F. Gorykin, G.V. Zaporozhan, A.K. Voitenko, Inzh.-Fiz. Zh. 29 (1975) 581–588.
[34] V.F. Chaikovskiy, V.Z. Geller, S.F. Gorykin, S.D. Artamonov, G.E. Bondar, S.I. Ivanchenko, L.R. Lenskiy, V.G. Peredriy, Teplofiz. Svoistva Zhidkostey, Collect Nauka, Moscow 1976, pp. 108–117.
[35] V.Z. Geller, V.A. Rabinovich, Teplofiz. Svoistva Veshchestv Mater., Collect., 9, Standards Publ., Moscow, 1976, pp. 147–161.
[36] A.I. Shestova, The Investigation of Thermal Conductivity of Freons of the Methane Type [Ph.D. Thesis]. Novosibirsk, USSR: Institute of Theoretical Physics, 1977.
[37] O.B. Zvetkov, Y.A. Laptev, A.I. Vasilkov, Mashinyi i Apparatyi Cholodilnoj, Kriogennoh Techniki i Kondizionirovaniyi Vosducha, Collect No. 2, Leningradskij Tech. Inst., 1977, pp. 54–56.
[38] T. Makita, Y. Tanaka, Y. Morimoto, M. Noguchi, H. Kubota, Int. J. Thermophys. 2 (1981) 249–268.
[39] M.D. Potapov, The Thermal Conductivity of Liquid Binary Mixturesof Halogenated Hydrocarbons [Ph.D. Thesis]. Odessa, USSR, Odessa Technological Institute of Food Industry, 1988.
[40] M. Papadaki, W.A. Wakeham, Int. J. Thermophys. 14 (1993) 1215–1220, doi:10.1007/bf02431285.
[41] A. Grebenkov, Y.G. Kotelevsky, V. Saplitza, O. Beljaeva, T. Zajatz, B. Timofeev, Experimental study of thermal conductivity of some ozone safe refrigerants and speed of sound in their liquid phase, CFCs: The Day After, Joint Meeting of IIR Commissions B1, B2, E1, and E2; Padova, Italy, 1994.
[42] M.J. Assael, L. Karagiannidis, Int. J. Thermophys. 16 (1995) 851–865, doi:10.1007/bf02093468.
[43] S.T. Ro, J.Y. Kim, D.S. Kim, Int. J. Thermophys. 16 (1995) 1193–1201, doi:10.1007/bf02081287.
[44] Y. Tanaka, S. Matsuo, S. Taya, Int. J. Thermophys. 16–16 (1995) 121–131, doi:10.1007/bf01438963.
[45] U. Gross, Y.W. Song, Int. J. Thermophys. 17 (1996) 607–619, doi:10.1007/bf01441507.
[46] J. Yata, M. Hori, K. Kobayashi, T. Minamiyama, Int. J. Thermophys. 17 (1996) 561–571, doi:10.1007/bf01441503.
[47] S.T. Ro, M.S. Kim, S.U. Jeong, Int. J. Thermophys. 18 (1997) 991–999, doi:10.1007/bf02575243.
[48] L.-Q. Sun, M.-S. Zhu, L.-Z. Han, Z.-Z. Lin, J. Chem. Eng. Data 42 (1997) 179–182, doi:10.1021/je960245k.
[49] B. Le Neindre, Y. Garrabos, Int. J. Thermophys. 22 (2001) 701–722, doi:10.1023/a:1010766730306.
[50] T. Tomimura, Netsu Bussei 15 (2001) 9–14.
[51] B. Fellows, R. Richard, I. Shankland, Thermal Conductivity 21 (1990) 311–325.
[52] A. Asambaev, Thermal conductivity of liquid and gaseous freons and their mixtures [Ph.D. Thesis]. St. Petersburg, Russia, Institute of Technology for Refrigiration Industry, 1992.
[53] L.C. Wilson, W.V. Wilding, G.M. Wilson, R.L. Rowley, V.M. Felix, T. Chisolmcarter, Fluid Phase Equilib. 80 (1992) 167–177, doi:10.1016/0378-3812(92)87065-u.
[54] O.B. Tsvetkov, Y.A. Laptev, A.G. Asambaev, Int. J. Thermophys. 15 (1994) 203–214, doi:10.1007/bf01441582.
[55] O.B. Tsvetkov, A.V. Kletski, Y.A. Laptev, A.J. Asambaev, I.A. Zausaev, Int. J. Thermophys. 16 (1995) 1185–1192, doi:10.1007/bf02081286.
[56] X. Gao, T. Yamada, Y. Nagasaka, A. Nagashima, Int. J. Thermophys. 17 (1996) 279–292, doi:10.1007/bf01443393.
[57] M.J. Assael, N. Malamataris, L. Karagiannidis, Int. J. Thermophys. 18 (1997) 341–352, doi:10.1007/bf02575165.
[58] S.U. Jeong, M.S. Kim, S.T. Ro, Int. J. Thermophys. 20 (1999) 55–62, doi:10.1023/a:1021469928377.
[59] B. Le Neindre, Y. Garrabos, Int. J. Thermophys. 20 (1999) 375–399, doi:10.1023/a:1022692601764.
[60] R.A. Perkins, M.L. Huber, J. Chem. Eng. Data 51 (2006) 898–904, doi:10.1021/je050372t.
[61] R.G. Richard, I.R. Shankland, Int. J. Thermophys. 10 (1989) 673–686, doi:10.1007/bf00507988.
[62] U. Gross, Y. Song, J. Kallweit, E. Hahne, Sci. Tech. Froid (1990) 103–108.
[63] G.Y. Ruvinskii, G.K. Lavrenchenko, S.V. Il'yushenko, Kholod. Tekhn. 67 (1990) 20–26.
[64] Y. Tanaka, M. Nakata, T. Makita, Int. J. Thermophys. 12 (1991) 949–963, doi:10.1007/bf00503512.

[65] Y. Ueno, Y. Nagasaka, A. Nagashima, The thermal conductivity of HCFC-123 and HFC-134a in the gaseous phase, Proc. Symp. Thermophys. Prop., 12th; Tokyo, Japan, 1991.
[66] U. Gross, Y.W. Song, E. Hahne, Int. J. Thermophys. 13 (1992) 957–983, doi:10.1007/bf01141209.
[67] A. Laesecke, R.A. Perkins, C.A.N.d. Castro, Fluid Phase Equilib. 80 (1992) 263–274.
[68] G.K. Lavrenchenko, G.Y. Ruvinskij, S.V. Iijushenko, V.V. Kanaev, Int. J. Refrigeration-Revue Internationale Du Froid 15 (1992) 386–392, doi:10.1016/0140-7007(92)90023-n.
[69] R.A. Perkins, A. Laesecke, C.A.N. Decastro, Fluid Phase Equilib. 80 (1992) 275–286, doi:10.1016/0378-3812(92)87074-w.
[70] M. Papadaki, M. Schmitt, A. Seitz, K. Stephan, B. Taxis, W.A. Wakeham, Int. J. Thermophys. 14 (1993) 173–181, doi:10.1007/bf00507806.
[71] R. Yamamoto, S. Matsuo, Y. Tanaka, Int. J. Thermophys. 14 (1993) 79–90, doi:10.1007/bf00522663.
[72] A.N. Gurova, T.G. Barao, C.A. Nieto de Castro, U.V. Mardolcar, High Temperatures-High Pressures 26 (1994) 25–34.
[73] D.S. Kim, J.Y. Kim, S.T. Ro, Thermal Conductivity 22 (1994) 177–188.
[74] U. Hammerschmidt, Int. J. Thermophys. 16 (1995) 1203–1211, doi:10.1007/bf02081288.
[75] M. Liu, L. Han, Y. Zhang, M. Zhu, J. Eng. Thermophysics (in Chinese) 3 (1995) 273–275.
[76] A.N. Gurova, U.V. Mardolcar, C.A.N. de Castro, Int. J. Thermophys. 18 (1997) 1077–1087, doi:10.1007/bf02575250.
[77] B. Le Neindre, Y. Garrabos, Int. J. Thermophys. 20 (1999) 1379–1401, doi:10.1023/a:1021480803361.
[78] R.A. Perkins, A. Laesecke, J. Howley, M.L.V. Ramires, A.N. Gurova, L. Cusco, NIST Interagency/Internal Report, NIST, Boulder, Colorado, 2000, doi:10.6028/nist.Ir.6605.
[79] B. Le Neindre, Y. Garrabos, F. Gumerov, A. Sabirzianov, J. Chem. Eng. Data 54 (2009) 2678–2688, doi:10.1021/je900210h.
[80] B. Le Neindre, Y. Garrabos, M.S. Kim, Int. J. Thermophys. 22 (2001) 723–748, doi:10.1023/a:1010718814377.
[81] S.H. Lee, M.S. Kim, S.T. Ro, J. Chem. Eng. Data 46 (2001) 1013–1015, doi:10.1021/je000230t.
[82] V.V. Slusarev, P.M. Kessel'man, Izv. Vyssh. Uchebn. Zaved., Neft Gaz 19 (1976) 109.
[83] V.V. Slusarev, The Investigation of the Thermal Conductivity of Freons of the Ethane Type of Fluorocarbons [Ph.D. Thesis]. Odessa, USSR, Institute of Technology for Food Industry, 1979.
[84] R. Afshar, S.C. Saxena, Int. J. Thermophys. 1 (1980) 51–59, doi:10.1007/bf00506271.
[85] V.Z. Geller, G.V. Zaporozhan, S.V. Ilushenko, Promyshlennaya Teplotekhnika 4 (1982) 77–80.
[86] U. Gross, Y.W. Song, E. Hahne, Fluid Phase Equilib. 76 (1992) 273–282, doi:10.1016/0378-3812(92)85094-o.
[87] J. Yata, M. Hori, T. Kurahashi, T. Minamiyama, Fluid Phase Equilib. 80 (1992) 287–296, doi:10.1016/0378-3812(92)87075-x.
[88] J.M. Yin, J.X. Guo, Z.Y. Zhao, L.C. Tan, M. Zhao, Fluid Phase Equilib. 80 (1992) 297–303, doi:10.1016/0378-3812(92)87076-y.
[89] S.H. Kim, D.S. Kim, M.S. Kim, S.T. Ro, Int. J. Thermophys. 14 (1993) 937–950, doi:10.1007/bf00502116.
[90] W.M. Haynes, Thermophysical Properties of HFC-143a And HFC-152a (DOE/CE/23810–39), Thermophysics Division, NIST, Boulder, Colorado, 1994.
[91] O.B. Tsvetkov, Y.A. Laptev, A.G. Asambaev, Int. J. Thermophys. 17 (1996) 597–606, doi:10.1007/bf01441506.
[92] A.N. Gurova, U.V. Mardolcar, C.A.N. de Castro, Int. J. Thermophys. 20 (1999) 63–72, doi:10.1023/a:1021422012447.
[93] B. Le Neindre, Y. Garrabos, High Temperatures-High Pressures 34 (2002) 307–314, doi:10.1068/htjr029.
[94] C. Yao, X. Zhao, S. Lv, Z. Guo, Fluid Phase Equilib. 375 (2014) 228–235, doi:10.1016/j.fluid.2014.04.038.
[95] R. Perkins, L. Cusco, J. Howley, A. Laesecke, S. Matthes, M.L.V. Ramires, J. Chem. Eng. Data 46 (2001) 428–432, doi:10.1021/je990337k.
[96] A.V. Baginskii, S.V. Stankus, Int. J. Thermophys. 24 (2003) 953–961, doi:10.1023/a:1025080212858.
[97] J. Pan, X. Li, J. Wu, Fluid Phase Equilib. 304 (2011) 64–67, doi:10.1016/j.fluid.2011.02.015.
[98] R. Dohrn, R. Treckmann, T. Heinemann, Fluid Phase Equilib. 158 (1999) 1021–1028, doi:10.1016/s0378-3812(99)00126-0.
[99] V. Geller, D. Bivens, A. Yokozeki, Transport properties and surface tension of hydrofluorocarbons HFC236fa and HFC245fa, 20th International Congress of Refrigeration: Refrigeration into the Third Millennium; Sydney Australia, 1999.
[100] J. Yata, M. Hori, M. Niki, Y. Isono, Y. Yanagitani, Fluid Phase Equilib. 174 (2000) 221–229, doi:10.1016/s0378-3812(00)00429-5.
[101] A.J. Grebenkov, O.V. Beliayeva, P.M. Klepatski, V.V. Saplitsa, B.D. Timofeyev, V.P. Tsurbelev, T.A. Zayats, ASHRAE Research Project, Joint Institute for Power and Nuclear Research, Sosny, Belarus, 2004.
[102] Y. Wang, J. Wu, Z. Xue, Z. Liu, J. Chem. Eng. Data 51 (2006) 1424–1428, doi:10.1021/je060116w.
[103] R.A. Perkins, M.L. Huber, M.J. Assael, J. Chem. Eng. Data 61 (2016) 3286–3294, doi:10.1021/acs.jced.6b00350.
[104] R.A. Perkins, M.L. Huber, J. Chem. Eng. Data 56 (2011) 4868–4874, doi:10.1021/je200811n.
[105] A.J. Grebenkov, Physical properties and equation of state for trans-1, 3, 3, 3-tetrafluoropropene, 3rd IIR Conference on Thermophysical Properties and Transfer Processes of Refrigerants; Boulder, Colorado, 2009.
[106] D. Kim, H. Liu, X. Yang, F. Yang, J. Morfitt, A. Arami-Niya, M. Ryu, Y. Duan, E.F. May, Int. J. Refrigeration, 2020, In preparation.
[107] I.H. Bell, J. Chem. Eng. Data 65 (2020) 5606–5616, doi:10.1021/acs.jced.0c00749.
[108] M. Binti Mohd Taib, J.P.M. Trusler, J. Chem. Phys. 152 (2020) 164104, doi:10.1063/5.0002242.
[109] S.J. Suresh, J.R. Elliott Jr., Ind. Eng. Chem. Res. 31 (1992) 2783–2794, doi:10.1021/ie00012a025.
[110] L. Monchick, K.S. Yun, E.A. Mason, J. Chem. Phys. 39 (1963) 654–669, doi:10.1063/1.1734304.
[111] X. Gao, Y. Nagasaka, A. Nagashima, Int. J. Thermophys. 20 (1999) 1403–1415, doi:10.1023/a:1021432920199.
[112] V.Z. Geller, B.V. Nemzer, U.V. Cheremnykh, Int. J. Thermophys. 22 (2001) 1035–1043, doi:10.1023/A:1010691504352.
[113] O.I. Verba, E.P. Raschektaeva, S.V. Stankus, Thermophysics and Aeromechanics 24 (2017) 135–139, doi:10.1134/s0869864317010140.
[114] D. Kim, X. Yang, A. Arami-Niya, D. Rowland, X. Xiao, S. Al Ghafri, T. Tsuji, Y. Tanaka, Y. Seiki, E.F. May, J. Chem. Thermodyn. (2020) 106248, doi:10.1016/j.jct.2020.106248.
[115] R.A. Perkins, E. Schawarzberg, X. Gao, NIST Interagency/Internal Report, NIST, Boulder, Colorado, 1999, doi:10.6028/nist.Ir.6605.
[116] A.V. Baginsky, A.S. Shipitsyna, Thermophysics and Aeromechanics 15 (2008) 291–295, doi:10.1134/s0869864308020121.
[117] S.K. Mylona, T.J. Hughes, A.A. Saeed, D. Rowland, J. Park, T. Tsuji, Y. Tanaka, Y. Seiki, E.F. May, J. Chem. Thermodyn. 133 (2019) 135–142, doi:10.1016/j.jct.2019.01.028.
[118] J.C. Dyre, J. Chem. Phys. 149 (2018) 210901, doi:10.1063/1.5055064.
[119] L. Costigliola, D.M. Heyes, T.B. Schroder, J.C. Dyre, J. Chem. Phys. 150 (2019) 021101, doi:10.1063/1.5080662.
[120] S. Kiselev, J. Ely, Fluid Phase Equilib. 252 (2007) 57–65, doi:10.1016/j.fluid.2006.10.028.
[121] F. Yang, Q. Liu, Y. Duan, Z. Yang, Fluid Phase Equilib. 494 (2019) 161–171, doi:10.1016/j.fluid.2019.04.035.
[122] F. Yang, Q. Liu, Y. Duan, Z. Yang, Chinese Science Bulletin (in Chinese) 64 (2019) 2741–2750, doi:10.1360/TB-2019-0159.
[123] J.A. White, S. Zhang, J. Chem. Phys. 103 (1995) 1922–1928, doi:10.1063/1.469716.
[124] X.-H. Xu, Y.-Y. Duan, Fluid Phase Equilib. 290 (2010) 148–152, doi:10.1016/j.fluid.2009.11.015.
[125] G.A. Olchowy, J.V. Sengers, Phys. Rev. Lett. 61 (1988) 15–18, doi:10.1103/PhysRevLett.61.15.
[126] P.M. Mathias, V.S. Parekh, E.J. Miller, Ind. Eng. Chem. Res. 41 (2002) 989–999, doi:10.1021/ie0102854.
[127] G. Galliero, C. Boned, J. Fernandez, J. Chem. Phys. 134 (2011) 064505, doi:10.1063/1.3553262.
[128] H. Liu, F. Yang, K. Zhang, Y. Duan, Z. Yang, J. Eng. Thermophys. (in Chinese) 42 (2021) 1–8.